

## **COMPUTATION OF HYDRODYNAMIC CHARACTERISTICS OF WATER FLOW IN ELECTRICAL SUBMERSIBLE PUMP**

**Mohammed K. Abbas<sup>1</sup>, Ali Z. Asker<sup>2</sup>, Samir D Ali.<sup>3</sup>**

Engineering Collage, Diyala University

<sup>1</sup>Mohammed\_70a@yahoo.com. <sup>2</sup>alichemolas@yahoo.com Assist.lecturer1960@yahoo.com

(Received:15/5/2011 ; Accepted:9/10/2011)

**ABSTRACT :-** The electrical submersible pump (ESP) systems play an important role in the industry and many engineering applications. It is frequently used in the drinking water purification units for lifting water from well. The centrifugal pump is the most important part of ESP systems. In the present work, a simulation have been carried out using Computational Fluid Dynamic CFD techniques and commercial software based on the finite volume method, ANSYS<sup>®</sup> CFX<sup>®</sup> Release 11.0. The results of the simulations include the pressure fields, velocity field, and velocity vector obtained to the internal flow in the impeller and diffuser channels of a centrifugal pump at flow rate 0.005m<sup>3</sup>/s. A stationary flow with constant boundary conditions is proposed. A comparison between the simulation of the present work and the head capacity of the performance curve that obtained practically was performed and showed satisfactory agreement.

**Key words:-** Computational Fluid Dynamic CFD, electrical submersible pump (ESP) systems, centrifugal pump, ANSYS<sup>®</sup>CFX<sup>®</sup> Release 11.0.

---

<b>Nomenclature</b>	<b>Description</b>	<b>Units</b>
P	The pressure	atm
$\rho$	Water density	kg/m <sup>3</sup>
$V_r, V_\theta, V_z$	Radial ,angular and axial velocity	
$\mu_{ef}$	Fluid effective viscosity	Pa·s
$\Gamma_c, \Gamma_\varepsilon$	Diffusion coefficients	

$\Phi$	Dissipation viscous rate in cylindrical coordinates	
$\mu$	Molecular viscosity	kg/m.s
$\mu_t$	Turbulent viscosity	kg/m.s

## INTRODUCTION

The Electrical Submersible pump (ESP) systems are increasingly used in many fields namely in drinking water purification systems. It is employed in Kanaan's city drinking water station as shown in figure (1). The ESP is used for lifting water with different flow rates from the bottom of the well to the ground surface to be treated. However, ESPs are always consists of two parts. The first comprised of an electric motor, seal section, gas separator, centrifugal pump and electric power cable. All this set runs into the well, protected by the casing. While the second part is positioned on the surface, the main components are the cable junction box, switchboard, motor controller and transformers. The centrifugal pumps are the heart of the system and are used in the ESP systems add power to the fluid to lift it toward the surface as use in Kanaan city drinking water purification station . The centrifugal pumps are composed of two main parts: an impeller (rotor) that rotates at the motor speed and imparts centrifugal forces to the production fluids and the diffuser (stator), which is the fixed part that guides the flow to the discharge.

The centrifugal pumps were studied by many authors. Cheah<sup>(1)</sup> studied the simulation in the complex internal flow in a centrifugal pump impeller with six twisted blades by using 3-D Navier-Stokes code with a standard k-  $\epsilon$  two-equation turbulence model , different flow rates were specified at inlet boundary to predict the characteristics of the pump .

Miguel<sup>(2)</sup> studied a 3-D-CFD simulation of the impeller and volute of a centrifugal pump has been performed using CFX codes, and calculate the velocity and pressure field for different flow rates of a centrifugal pump, allowing to obtain the radial thrust on the pump shaft.

John<sup>(3)</sup> studied the simulation of the three-dimensional turbulent flow in the turbomachines based on the solution of the Reynolds Averaged Navier Stokes equations, and he use the cartesian grids combined with a numerical technique for solving partially blocked cells.

Kergourlay <sup>(4)</sup> studied the influence of adding splitter blades on the performance of a hydraulic centrifugal pump, the sliding mesh method is used to model the rotor zone motion in order to simulate the impeller-volute casing interaction and compute velocity and pressure fields using unsteady Reynolds-averaged Navier- Stokes approach at different flow rates.

Tran H. <sup>(5)</sup> studied the numerical modeling of the flow through the impeller and volute using CFD code (FLUENT Vr. 6.3) to investigate the flow in a complex geometry of a centrifugal pump to predict the achievable head and capacity.

Maitelli <sup>(6)</sup> studied a 3-D simulation of the stationary flow in the impeller and stator of a mixed centrifugal pump using computational fluid dynamics (CFD) techniques and a commercial software, ANSYS<sup>®</sup> CFX<sup>®</sup> Release 11.0, three conditions were simulated to obtain the pressure fields in the impeller and stator in a stage of the pump.

Lamloumi <sup>(7)</sup> studied the viscous Navier-Stokes equations to simulate the flow inside the impeller and volute, and develop a method to obtain three-dimensional velocity and pressure distribution within a centrifugal pump. The method is based on solving fully elliptic partial differential equations for the conservation of mass and momentum.

Weidong <sup>(8)</sup> described the three-dimensional simulation of internal flow in three different types of centrifugal pumps. He used a 3-D Navier-Stokes equation, finite volume method, with the aid of ANSYS<sup>®</sup> CFX<sup>®</sup> with a standard k- $\epsilon$  two-equation turbulence model to simulate the problem.

Gonzalez J. <sup>(9)</sup> studied the numerical simulation by using the viscous Navier-Stokes equations in capturing the dynamic and unsteady flow effects inside a commercial centrifugal water pump with backward curved blades to obtain the effects of the blade passage in front of the tongue and both the flow and pressure fluctuations.

Bacharoudis E. <sup>(10)</sup> studied the numerical solution of the discretized three-dimensional, incompressible Navier-Stokes equations over an unstructured grid is accomplished with a commercial CFD finite volume code to obtain the performance of the impellers with the same outlet diameter having different outlet blade angles.

The objective of this work is to simulate the water flow in submersible pump. The simulation include the pressure, velocity and velocity vectors distributions of the internal flow in the impeller and diffuser channels of the submersible pump and plotting several variable contours on profiles view. Besides comparing the head-flow curve of the submersible pump between that was obtained by simulation with the experimental one of Kannan's city drinking water purification system.

## SPECIFICATION OF THE PUMP

The centrifugal pump operation is very simple. The design of the submersible centrifugal pumps fall into two general categories. It comprised of an electric motor, electric power cable and centrifugal pump. All this set runs into the well, protected by the casing. On the surface, the main components are the cable junction box, switchboard, motor controller and transformers which shown in figure (1). The centrifugal pumps are composed of impeller and diffuser as shown in figure (2). It is the heart of the system and used in the ESP systems to add power to the fluid to lift it toward the surface in agreement with the capacity to be pumped. ESP pumps can be applicable to a wide range of flow rates. The geometrical specifications of the pump which used in the model were shown in table (1).

## MATHEMATICAL FORMULATION

The three-dimensional and incompressible steady flow, the continuity and momentum equations can be written in the cylindrical coordinates for radial, angular and axial directions as follows: <sup>(6, 10)</sup>

$$\frac{1}{r} \frac{\partial(\rho r V_r)}{\partial r} + \frac{1}{r} \frac{\partial(\rho V_\theta)}{\partial \theta} + \frac{\partial(\rho V_z)}{\partial z} = 0 \dots \dots \dots (1)$$

r component

$$\rho \left( V_r \frac{\partial V_r}{\partial r} + \frac{V_\theta}{r} \frac{\partial V_r}{\partial \theta} + V_z \frac{\partial V_r}{\partial z} - \frac{V_\theta^2}{r} \right) = -\frac{\partial p}{\partial r} + \mu \left\{ \frac{\partial}{\partial r} \left[ \frac{1}{r} \frac{\partial(r V_r)}{\partial r} \right] + \frac{1}{r^2} \frac{\partial^2 V_r}{\partial \theta^2} + \frac{\partial^2 V_r}{\partial z^2} - \frac{2}{r^2} \frac{\partial V_\theta}{\partial \theta} \right\} + F_r \dots \dots \dots (2)$$

θ Component

$$\rho \left( V_r \frac{\partial V_\theta}{\partial r} + \frac{V_\theta}{r} \frac{\partial V_\theta}{\partial \theta} + \frac{V_\theta V_r}{r} + V_z \frac{\partial V_\theta}{\partial z} \right) = -\frac{1}{r} \frac{\partial p}{\partial \theta} + \mu \left\{ \frac{\partial}{\partial r} \left[ \frac{1}{r} \frac{\partial(r V_\theta)}{\partial r} \right] + \frac{1}{r^2} \frac{\partial^2 V_\theta}{\partial \theta^2} + \frac{\partial^2 V_\theta}{\partial z^2} + \frac{2}{r^2} \frac{\partial V_r}{\partial \theta} \right\} + F_\theta \dots \dots \dots (3)$$

z component

$$\rho \left( V_r \frac{\partial V_z}{\partial r} + \frac{V_\theta}{r} \frac{\partial V_z}{\partial \theta} + V_z \frac{\partial V_z}{\partial z} \right) = -\frac{\partial p}{\partial z} + \mu \left\{ \frac{1}{r} \frac{\partial}{\partial r} \left[ \frac{r V_z}{\partial r} \right] + \frac{1}{r^2} \frac{\partial^2 V_z}{\partial \theta^2} + \frac{\partial^2 V_\theta}{\partial z^2} + \frac{\partial^2 V_z}{\partial z^2} \right\} + F_z \dots \dots \dots (4)$$

The left side term in equations above represent the convective acceleration.

The right side terms represent the pressure gradient, the viscous effects and the source terms respectively. The turbulence model chosen was the  $k-\varepsilon$  model. It has widespread application in commercial software and robustness. The  $k-\varepsilon$  model and its extensions resolve the partial differential equations for turbulent kinetic energy  $k$  and the dissipation rate  $\varepsilon$  as given by the equations (5) and (6):

$$\rho [\vec{V} \cdot (\nabla k)] = \nabla \cdot (\Gamma_c \nabla k) + P - \rho \varepsilon \dots \dots \dots (5)$$

$$\rho [\vec{V} \cdot (\nabla \varepsilon)] = \nabla \cdot (\Gamma_\varepsilon \nabla \varepsilon) + C_{\varepsilon 1} \frac{\varepsilon P}{k} - C_{\varepsilon 2} \frac{\rho \varepsilon^2}{k} \dots \dots \dots (6)$$

$$\Gamma_c = \mu + \frac{\mu_t}{\sigma_k} \dots \dots \dots (7)$$

$$\Gamma_\varepsilon = \mu + \frac{\mu_t}{\sigma_\varepsilon} \dots \dots \dots (8)$$

The term  $C_{\varepsilon 1}$ ,  $C_{\varepsilon 2}$ ,  $\sigma_k$ , and  $\sigma_\varepsilon$  in equations 6, 7 and 8 are constant in  $k-\varepsilon$  turbulence model and their values are  $C_{\varepsilon 1}=1.44$ ;  $C_{\varepsilon 2}=1.92$ ;  $\sigma_k=1$  and  $\sigma_\varepsilon=1.3$ .

Then the pressure can be calculate as,

$$P = \mu_{ef} \Phi \dots \dots \dots (9)$$

$$\mu_{ef} = \mu + \mu_t \dots \dots \dots (10)$$

$$\mu_t = C_\mu \rho \frac{k^2}{\varepsilon} \dots \dots \dots (11)$$

Where  $C_\mu$  is constant =0.09.

## **SIMULATION CONSIDERATIONS AND BOUNDARY CONDITION**

The three-dimensional flow simulations were performed in the commercial software, based on CFD techniques, ANSYS® CFX® release 11.0. In the present study, the water considered to be one component single phase flow, at standard conditions and has physical properties shown in table (2). The impeller rotational speed was set at 3600 rpm. The reference pressure was adjusted to one atmosphere. The boundary conditions were set as follows: a total uniform pressure of one atmospheric at inlet and variable mass flow rate was considered at the outlet. These choices have resulted in robust and right solutions in the scope of the computational tool utilized. The summary of the boundary conditions of turbulence model  $k-\varepsilon$  are given in Table (3).

The meshes were generated by ANSYS<sup>(R)</sup> CFX<sup>(R)</sup> 11.0 with wedge elements, pyramid elements and tetrahedral elements in a non-structured mesh 86320 elements for the impeller and 112647 elements for the diffuser as shown in figures (4 and 5). The choice for the interface between the impeller and the diffuser was frozen rotor, typical for turbomachines in ANSYS® CFX® 11.0, specific for the steady state flow regime and composed structures with a rotative part (the impeller) and a fixed part (the diffuser).<sup>(11, 12)</sup>

## **RESULTS AND DISCUSSION**

The system of water purification (drinking water) of Kanaan's city in the field was shown in the figure (1). The relation between the head and the flow rate was given in the figure (3). The figure shows a comparison between the experimental and simulation results, the experimental data was collected from gauges of the experimental rig. It is obvious that the curve that was obtained by CFD model have the same tendency of behavior for the experimental case with a bit difference, this is due to friction losses. Figures (4) and (5) show the mesh distribution in the meridional profiles of diffuser and impeller channels respectively. That profile was obtained based on non-structured 86320 elements mesh for the impeller and 112647 elements for the diffuser.

The contour of fluid velocity in diffuser and impeller channels at a volumetric flow rate  $0.005\text{m}^3/\text{s}$  was given in the figures (6) and (7) respectively. The figures show that the velocity minimizes at the edges, and then it decreases towards the exit of the blade passage. Increased flow velocity can be observed at the blade inlet due to the blockage of the flow, whereas on the contrary the pressure is reduced. Further downstream the pressure contours become smooth between the blades and its value increases continuously towards the exit of

the computational domain <sup>(13)</sup>. While the figures (8) and (9) illustrates the contour of pressure distribution in diffuser and impeller at the same volumetric flow rate. It can be observed that the values of pressure obtained in the outlet impeller were about (252.5 kN/m<sup>2</sup>) and diffuser (250 kN/m<sup>2</sup>) entrance is continuous at the interface. This fact is an evidence of the interaction between the two structures and their meshes, i.e. the rotated impeller and the fixed diffuser.

Figures (10) and (11) show the contour of velocity vectors distribution in diffuser and impeller at volumetric flow rate 0.005 m<sup>3</sup>/s. When the flow rate is nominal or more than nominal, the fluid flows smoothly through the impeller passage. <sup>(10)</sup>

## **CONCLUSION**

In this paper a computational simulation of the centrifugal pump internal flow was implemented. A CFD code, the ANSYS<sup>®</sup> CFX<sup>®</sup> 11.0, was used to obtain the head performance curve which was gained by utilizing the software ability, and evaluate the interface connection between the pump parts: the impeller and the diffuser. The results obtained for the pressure fields, fluid velocity and velocity vector for impeller and diffuser channels and obtain the experimental results and compared with simulation which is adapter. The simulation was performed with the entire pump the pressure in the impeller channels increases from the entrance to the discharge in successive ranges. This fact shows the energy transfer in the impeller. In the impeller outlet, an elevation in the pressure values is observed. This actually means that the fluid displacement occurs due to the rotational movement of the fluid. The losses at the interface between the impeller and the diffuser can be noticed in this case.

## **REFERENCE**

1. Cheah K.W. 2007 "Numerical Flow Simulation in a Centrifugal Pump at Design and Off-Design Conditions" International Journal of Rotating Machinery, Volume, Article ID 83641, 8 pages.
2. Miguel A.2005" Numerical Modelization of the Flow in Centrifugal Pump: Volute Influence in Velocity and Pressure Fields" International Journal of Rotating Machinery, Vol 3, pp 244–255.

3. John S. 2006 "Numerical Calculation of the Flow in a Centrifugal Pump Impeller Using Cartesian Grid" Proceedings of the 2nd WSEAS Int. Conference on Applied and Theoretical Mechanics, Venice, Italy, November 20-22.
4. Kergourlay G. 2007" Influence of Splitter Blades on the Flow Field of a Centrifugal Pump: Test-Analysis Comparison" International Journal of Rotating Machinery Volume, Article ID 85024, 13 pages.
5. Tran H. 2008" Numerical Modeling as a Tool of Centrifugal Pump Q~H Curve Investigation" Proceedings of the scientific work of the VSB - Technical University of Ostrava.
6. Maitelli, C. 2010" Simulation of Flow in A Centrifugal Pump of ESP Systems Using Computational Fluid Dynamics "Brazilian journal of petroleum and gas, Vol 4, pp 1-9.
7. Lamloumi H. 2010" Numerical Flow Simulation in a Centrifugal Pump" International Renewable Energy Congress November 5-7, Sousse, Tunisia.
8. Weidong Z.2003" Investigation of Flow Through Centrifugal Pump Impellers Using Computational Fluid Dynamics" International Journal of Rotating Machinery, Vol 9 pp 49–61.
9. Gonzalez J.2002" Numerical Simulation of the Dynamic Effects Due to Impeller-Volute Interaction in a Centrifugal Pump" ASME, Journal of Fluids Engineering, June Vol. 124 pp 348-355.
10. Bacharoudis E.C 2008" Parametric Study of a Centrifugal Pump Impeller by Varying the Outlet Blade Angle "The Open Mechanical Engineering Journal, 2, pp 75-83.
11. ANSYS CFX-Reference Guide, ANSYS CFX Release 11.0 United States, December, 2006, Software handbook, P 934.
12. ANSYS CFX - Solver Modeling Guide, ANSYS CFX Release 11.0 United States, December, 2006,Software handbook, P 566 .
13. JOHN S.2006" Numerical Calculation of the Flow in a Centrifugal Pump Impeller Using Cartesian Grid" Conference on Applied and Theoretical Mechanics, Venice, Italy, November 20-22.

**COMPUTATION OF HYDRODYNAMIC CHARACTERISTICS OF WATER FLOW IN  
ELECTRICAL SUBMERSIBLE PUMP**

---

**Table (1):** Pump geometric characteristics

impeller inlet radius	16	mm
impeller outlet radius	36	mm
impeller inlet blade angle	30°	
impeller outlet blade angle	42°	
impeller inlet height	11	mm
impeller outlet height	6.5	mm
total impeller height	60	mm
total diffuser height	58	mm
total height, impeller and diffuser	63	mm
diffuser external diameter	88	mm

**Table (2):** Physical property of water .

Property of water	value
density	1000 kg / m <sup>3</sup>
Specific heat	4.18 kJ/kg.C
Thermal conductivity	0.556 W/m.C
Viscosity	9.8×10 <sup>-4</sup> kg / m.s

**Table (3):** Simulation parameters and boundary conditions.

Simulation parameters	boundary conditions (CFX values)
Mesh	Non –structured 86320 elements for the impeller and 112647 elements for the diffuser
Inlet total pressure	1 atm
Outlet mass flow rate	Variable (kg/s)
Slip the walls	No slip
Flow regime	Steady state
Turbulence model	<i>k-ε</i> .
Rotational speed	3600 rpm
Periodicity	Symmetrical surfaces in the middle of the channel between two blades
Walls	Solid walls not crossing the fluid
Impeller and diffuser interface	Frozen rotor



Fig. (1): Kanaan city drinking water purification station.



Fig.(2): Impeller and diffuser for ESP.

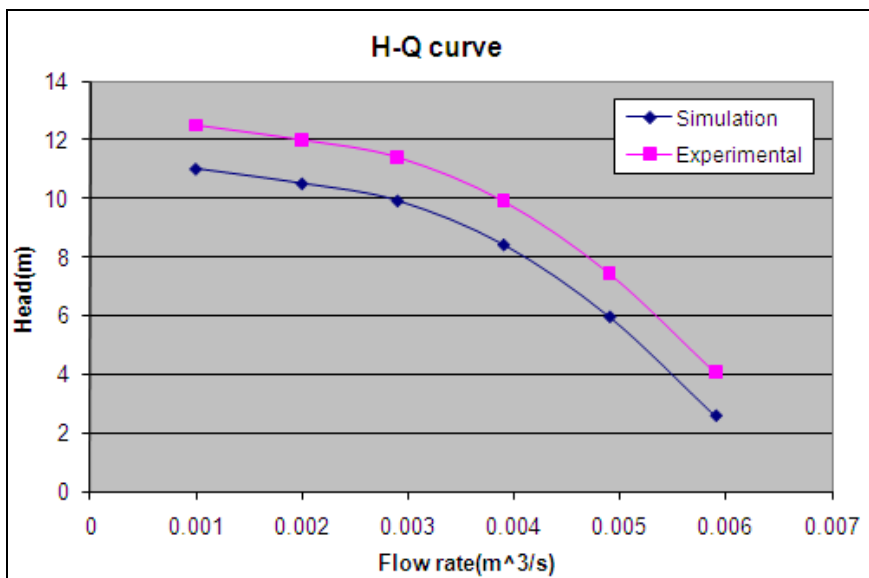


Fig.(3): Experimental and simulations results.

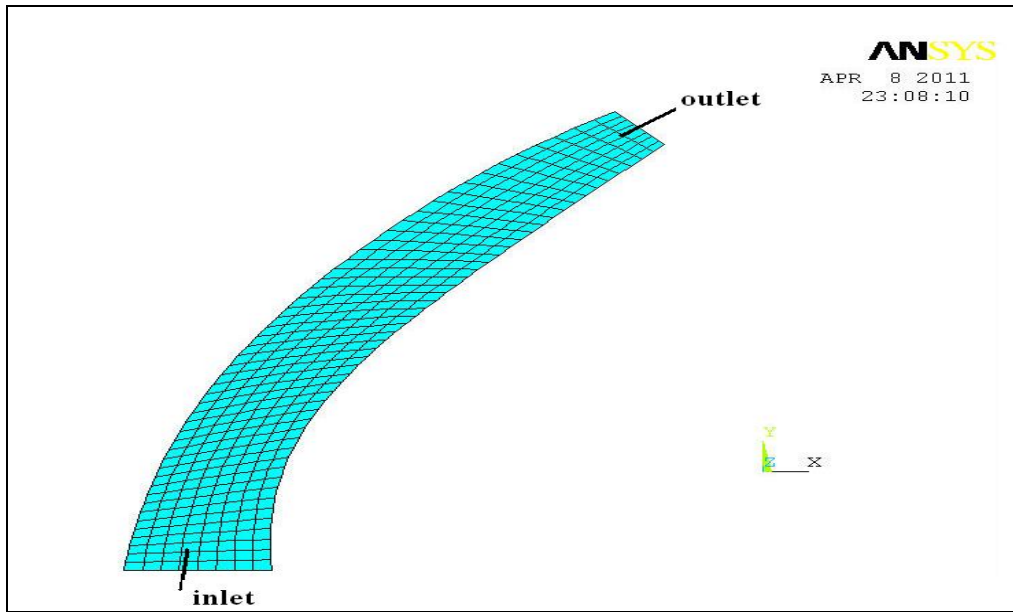


Fig.(4): diffuser channel mesh.

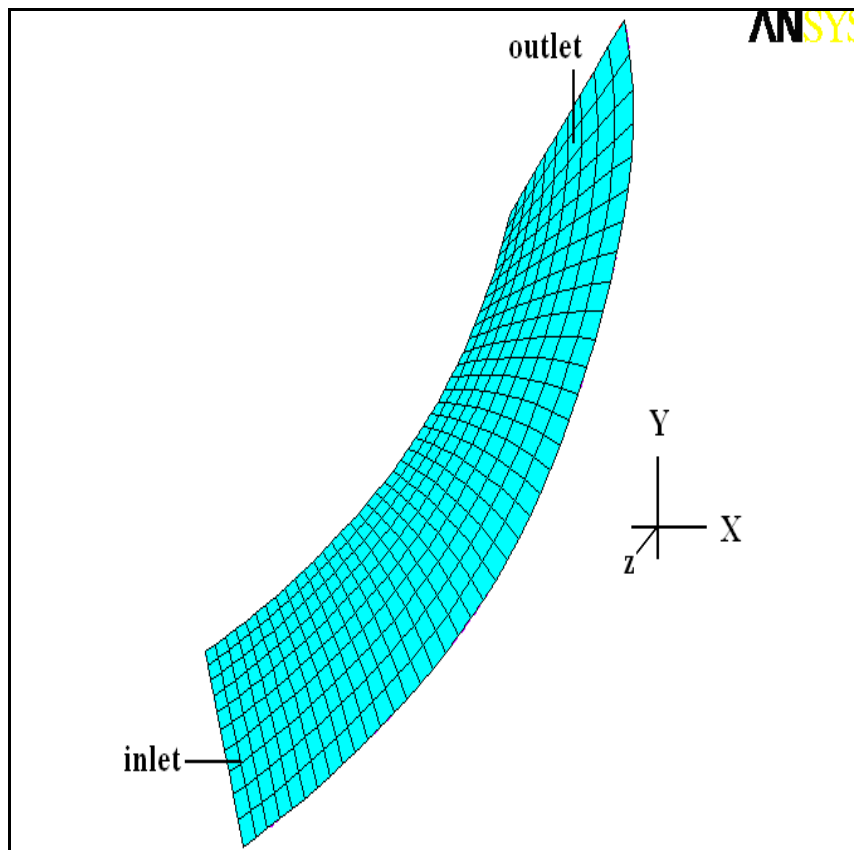
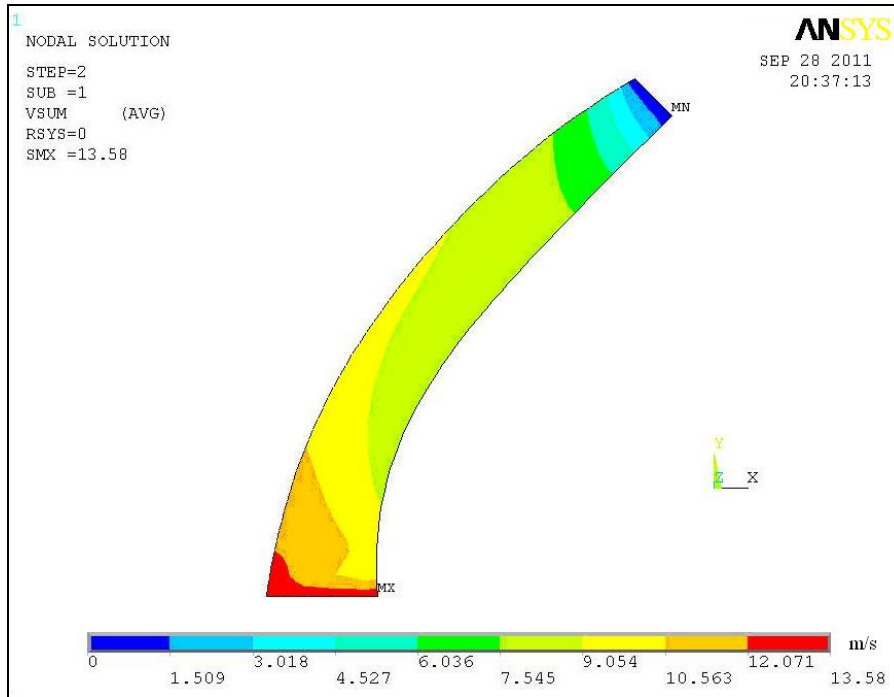
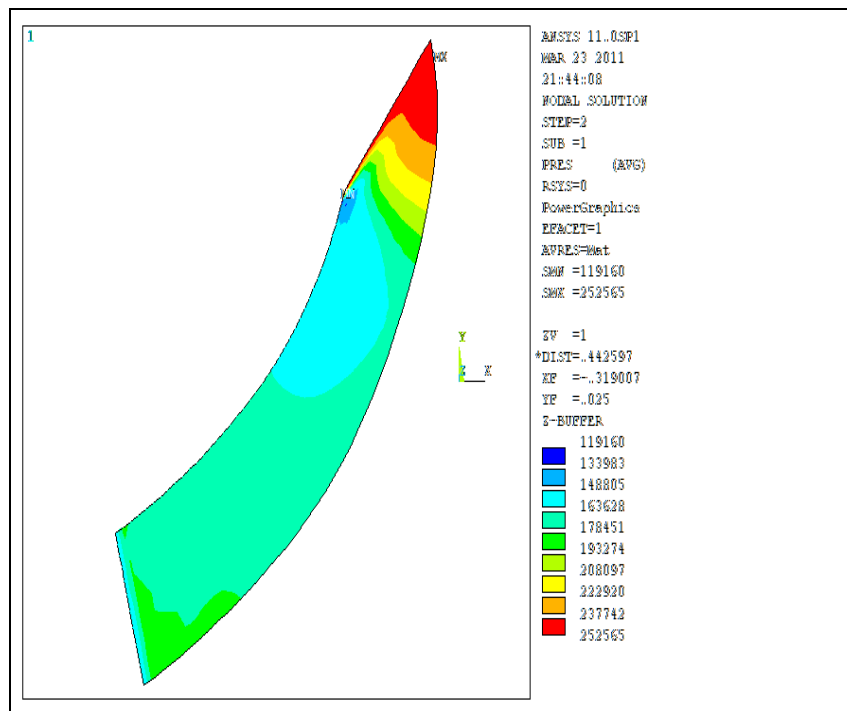


Fig. (5): Impeller channel mesh.

**COMPUTATION OF HYDRODYNAMIC CHARACTERISTICS OF WATER FLOW IN ELECTRICAL SUBMERSIBLE PUMP**



**Fig. (6):** Fluid velocity contour in diffuser at volumetric flow rate  $0.005 \text{ m}^3 / \text{s}$ .



**Fig. (7):** Fluid velocity contour in impeller at volumetric flow rate  $0.005 \text{ m}^3 / \text{s}$ .

**COMPUTATION OF HYDRODYNAMIC CHARACTERISTICS OF WATER FLOW IN ELECTRICAL SUBMERSIBLE PUMP**

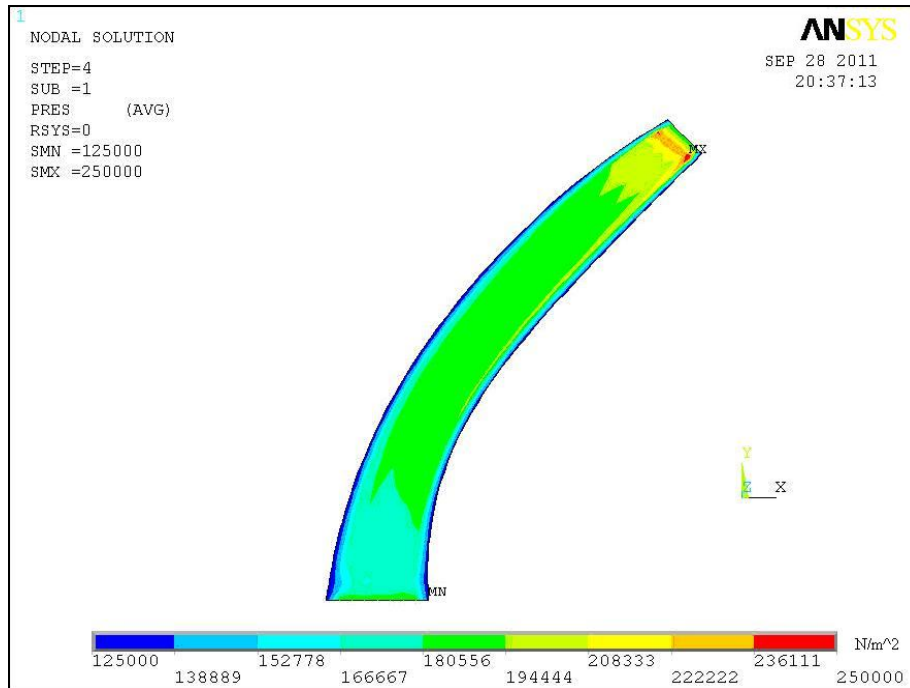


**Fig. (8):** Pressure distribution in diffuser at volumetric flow rate  $0.005 \text{ m}^3 / \text{s}$  .

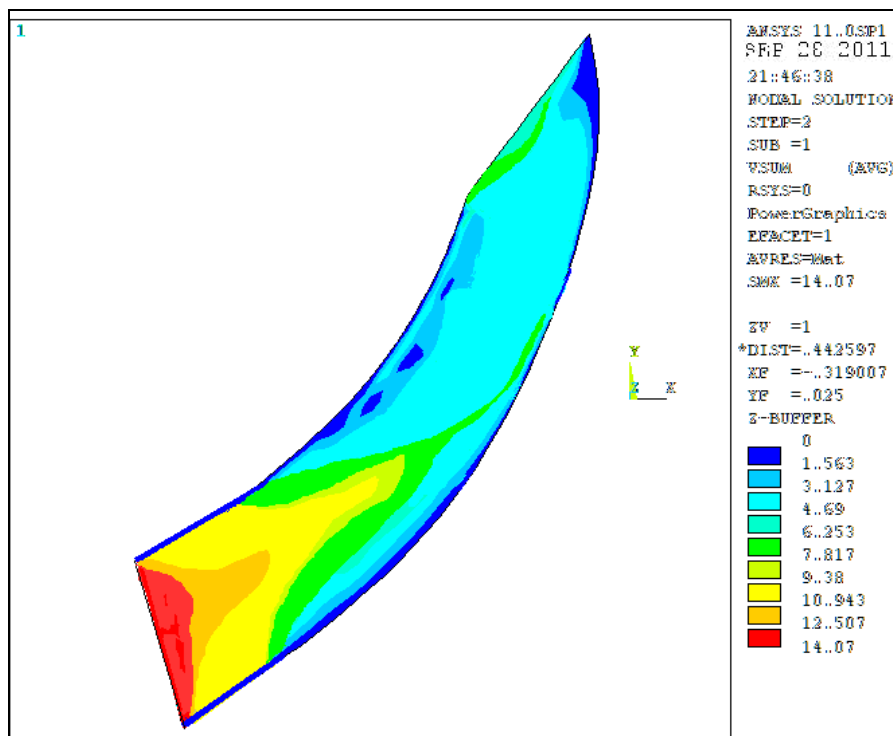


**Fig.(9):** Pressure distribution in impeller at volumetric flow rate  $0.005 \text{ m}^3 / \text{s}$  .

COMPUTATION OF HYDRODYNAMIC CHARACTERISTICS OF WATER FLOW IN ELECTRICAL SUBMERSIBLE PUMP

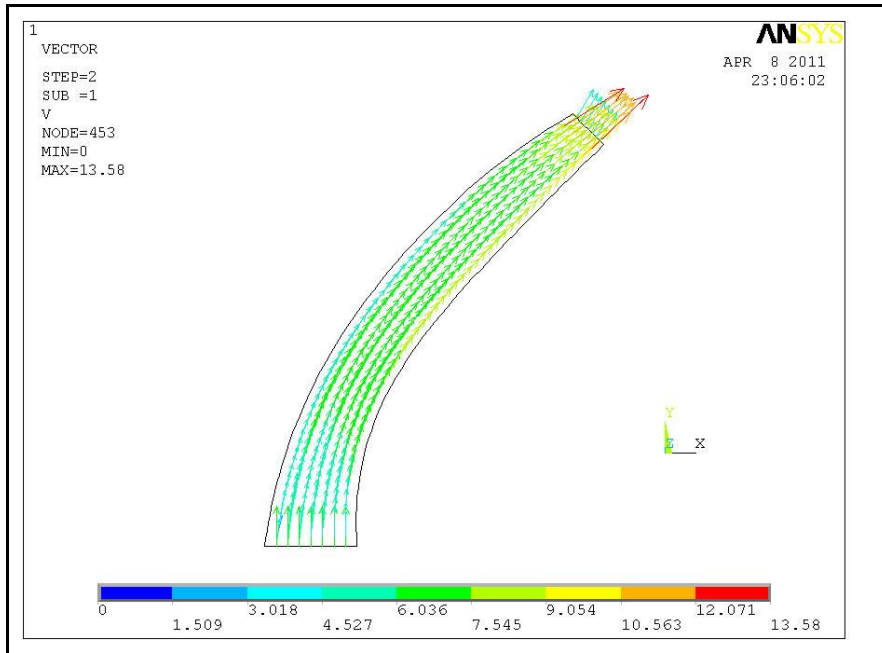


Fig. (10): Velocity vector distribution in diffuser at volumetric flow rate  $0.005 \text{ m}^3 / \text{s}$ .

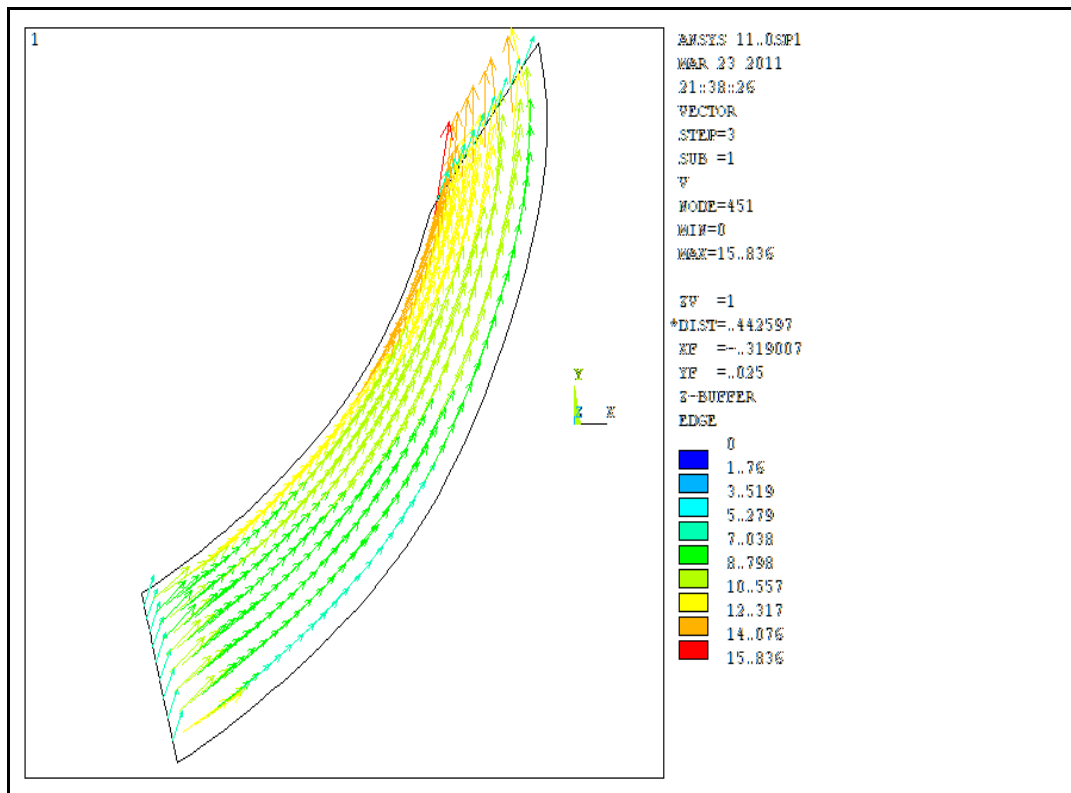


Fig. (11): Velocity vectors distribution in Impeller at volumetric flow rate  $0.005 \text{ m}^3 / \text{s}$ .

## حساب المعالم الهيدروديناميكية لجريان الماء في انظمة المضخات الكهربائية الغاطسة

م.م محمد خضير عباس      م.م علي زين العابدين عسكر      م.م سمير داود علي  
مدرس مساعد      مدرس مساعد      مدرس مساعد  
قسم الهندسة الميكانيكية - كلية الهندسة - جامعة ديالى

### الخلاصة:-

ان نظام المضخة الكهربائية الغاطسة (ESP) تلعب دورا هاما في الصناعة والعديد من التطبيقات الهندسية. وهي كثيرا ما تستخدم في وحدات تنقية مياه الشرب لرفع المياه من بئر. ان مضخة الطرد المركزي هي أهم جزء في نظم (ESP). في هذا العمل ، نفذت محاكاة باستخدام التقنيات الحاسوبية لديناميك المائع الحسابي CFD والبرمجيات التجارية على أساس أسلوب حجم محدود ، ANSYS® CFX® الاصدار 11.0 .

نتائج المحاكاة تشمل مجالات الضغط ، مجال السرعة للتيار في قنوات الجزء الدوار والناشر لمضخة طرد مركزي عند جريان 0.005 م<sup>3</sup>/ثانية تم افتراض شروط حدية ثابتة. وكانت النتائج التي تم الحصول عليها عن طريق المحاكاة لمخطط الضغط والجريان مقارنة للنتائج العملية التي تم استحصالها من محطة كنعان لتنقية مياه الشرب.

**الكلمات الدالة:-** ديناميك المائع الحسابي .المضخات الكهربائية الغاطسة . مضخة الطرد المركزي . ANSYS® CFX11